Study of a Three-Groove Kinematic Coupling for Precise Positioning in a Robotized Laser-Cutting Machine

Study of a three-groove kinematic coupling for precise positioning in a robotized laser-cutting machine

Carlo De Benedictis* and Carlo Ferraresi

Department of Mechanical and Aerospace Engineering, Politecnico di Torino, Italy
carlo.debenedictis@polito.it

Abstract. In this work, the positioning accuracy allowed by a three-groove kinematic coupling in a laser-cutting machine is studied. Kinematic couplings are designed to allow for improved accuracy and repeatability as compared to traditional elastic mediated coupling systems. A method for the estimation of positioning accuracy in a three-groove V-shaped coupling is reported, and the results of the analysis carried out on a multi-purpose laser-cutting machine are presented. The results confirm that a positioning error lower than 0.02 mm is ensured by the coupling in any tested condition.

Keywords: Three-groove coupling, kinematic coupling, precise positioning, machine design.

1 Introduction

In robotic systems where automatic operations are carried out, it is often required to ensure a high-precision coupling between two parts that need to be positioned relatively. Nowadays, the designers have pushed the performance of the most common couplings used in manufacturing (elastic deformation methods) to the limit accuracy of about five microns.

The simplest coupling design consists of surface contact, which generally occurs with direct contact between large and relatively flat interface elements. Alignment pins have long been considered the simplest and least expensive method for aligning components [1]. If there is no clearance, that is, if there is a pressure mount between the pin and the hole, they fall into the category of couplings with elastic deformation [2]. The manufacture of precision couplings is expensive because the positioning of the centers and the sizing of the components must be subjected to tolerances that are more restrictive than the repeatability required by the coupling. Methods based on elastic deformation such as wedges, guides and grooves, dovetail joints, and pressure joints achieve forced couplings of an over-determined type, that is, with redundancy of constraints. In such condition, a good repeatability is achieved only at the end of a so-called wear-in phase. When a high load capacity is required, interface couplings can be designed with the appropriate contact area to achieve a rigid joint.

Kinematic couplings are static, structural, precision machined contacts used to precisely locate components relative to each other [2-5]. They are designed in such a way

that the number of points of contact between two solid models corresponds to the number of degrees of freedom that are constrained. The coupling elements must be designed with great care and precision so that they can withstand high contact stresses at these points and maintain the integrity of the surface after repeated cycles [6,7]. Repeatability can be very high, with errors lower than 1 micron.

In this work, a method aimed at determining the positioning accuracy guaranteed by a three-groove kinematic coupling is applied to a precision laser-cutting robotized machine. In particular, balancing is discussed to further improve the accuracy of the system for the several loading conditions allowed by the machine. In the following, a presentation of the main features of the machine is given. Then, the analysis of the kinematic coupling is carried out and the results are shown.

2 The laser-cutting machine

The study was developed within a project developed by a company that is among the world leaders in the field of high-power laser-cutting and welding for industrial applications [8]. A CAD model of the machine is shown in Fig. 1.

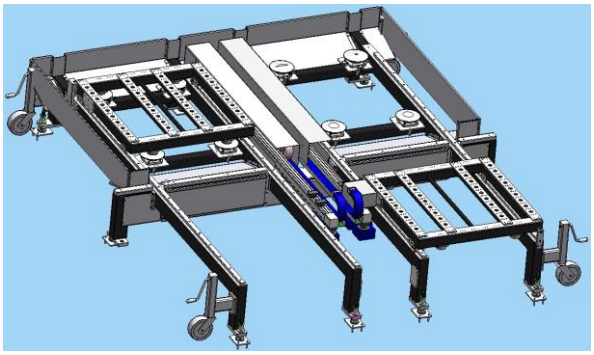

Fig. 1. The machine CAD model.

The machine consists of two independent modules located side by side. Each of these modules is mounted on a cart that translates along parallel routes between the workpiece loading station and the machining station, dragged by a gear motor mounted on a linear guide. At the four corners of the structure, height adjustable wheels are mounted to allow movement in the working area.

Once the working position is reached, the cart is decoupled from the guide and the vertical motion necessary to obtain the final positioning of the workpiece is allowed. The final positioning will be on the coupling elements only, so as to guarantee the required levels of precision (set as 0.02 mm by design specifications. The vertical movement is controlled by the inflation/deflation of two air springs for industrial applications interposed between the rails and the plane below (see Fig. 2). The elasticity of the air spring does not guarantee a straight vertical motion; therefore, side linear guides are required.

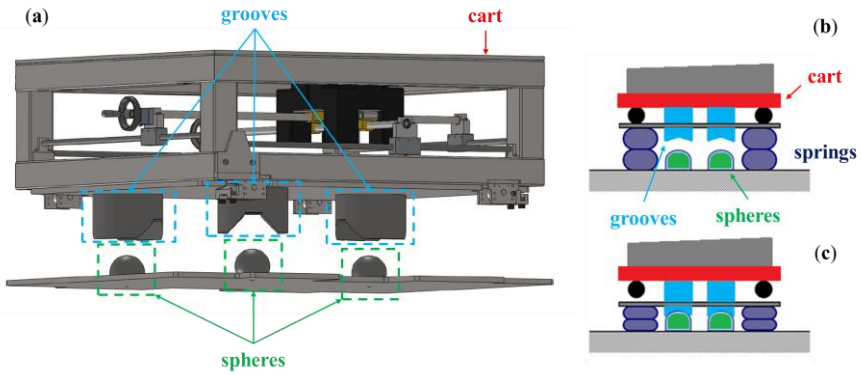

Fig. 2. Detail of the kinematic coupling: (**a**) CAD model; coupling in disengaged (**b**) and engaged (**c**) configurations.

3 Positioning accuracy of a three-groove kinematic coupling

The final coupling takes place through a structure including three balls and three V-grooves [9,10] (Fig. 2), mounted at the vertices of an equilateral triangle (see Fig. 3). The ball element, which is actually a spherical shell with a base at 3/4 of the total height, has a diameter of 100 mm. On its flat surface a threaded hole is drilled for connection to the fixed base. This solution implies that the spheres are fixed, whereas the grooves are integral with the moving cart (see Fig. 2). Each groove is a cylinder with diameter of 200 mm and height of 127.5 mm. On one side, contact surfaces are carved, inclined 90° relative to each other. Between the two surfaces, there are housings for two fixing screws. As far as the materials are concerned, the performance of a hardened stainless steel (440C SST), tungsten carbide (WC), Teflon, and a ceramic (Si3N4) were compared. To have smaller dimensions and lower production costs, 440C stainless steel was chosen.

The design of the coupling requires calculating the stresses and deflections at the contact, which affect the positioning error allowed by the kinematic coupling. Below, the most significant steps of this methodology are reported [9]. It starts from the knowledge of the following data: diameters of the spheres and radii of curvature of the grooves; the coordinates of the contact points of the spheres in the grooves; the orientations of the contact forces; the coordinates of the points of application of the preload forces; the preload forces on each ball/groove; the coordinates and components of an applied external load; the modulus of elasticity and Poisson coefficients of materials. To fulfill the theoretical stability requirement, for precise three-V kinematic couplings, stability and good overall stiffness will be ensured if the normals to the planes containing the contact force vectors for each ball bisect the internal angles between two adjacent sides of the coupling triangle. For instance, by considering the representation of Fig. 3, the normal to the π plane containing the contact force vectors for ball 2 must bisect the angle between the sides 12 and 23 (numbers refer to the spheres' nomenclature).

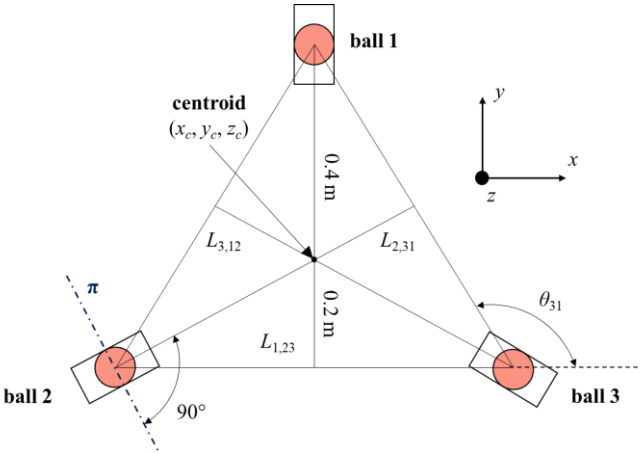

Fig. 3. Geometry of three-groove planar kinematic coupling.

By static analysis of the external forces F_e and moments M_e acting on the system, the calculation of the six contact forces F_{b_i} at the ball-groove interfaces can be derived (Eq. 1).

$$\sum \vec{F_e} = \vec{0}, \sum \vec{M_e} = \vec{0} \quad \longrightarrow \quad F_{b_i}, \quad (i = 1 \ldots 6) \tag{1}$$

Once the forces are known, they can be used to determine the stresses and deformation at the points of contact using Hertz's theory. The equivalent modulus of elasticity E for each ball/groove is first determined, then the equivalent radius R of the system (Eq. 2) is calculated:

$$E = \frac{1}{\frac{\left(1-\nu_g^{\,2}\right)}{E_g} + \frac{\left(1-\nu_b^{\,2}\right)}{E_b}}, \quad R_e = \frac{1}{\frac{1}{R_{g_{\max}}} + \frac{1}{R_{g_{\min}}} + \frac{1}{R_{b_{\max}}} + \frac{1}{R_{b_{\min}}}} \tag{2}$$

where $R_{b_{\max}}$ and $R_{b_{\min}}$ are equal, while for the groove $R_{g_{\max}}$ tends to infinity and $R_{g_{\min}}$ is negative. The modulus of elasticity and Poisson coefficients are provided both for balls, E_b and ν_b, and grooves, E_g and ν_g. The factor $cos\theta$, necessary for the calculation of the contact region (which will be an ellipse, see Fig. 4) according to the Hertzian theory, is equal to $R_e/|R_{g_{\min}}|$. Having calculated the semi-major and semi-minor axes of the ellipse $R_{\max}$ and $R_{\min}$, the Hertzian contact stress q and deflection δ can be determined for each ball, as reported in Eq. 3:

$$q = \frac{3F}{2\pi R_{\max} R_{\min}}, \quad \delta = \lambda \left(\frac{2F^2}{3R_e E_e^{\,2}} \right)^{1/3} \tag{3}$$

where F is the overall external force and λ is one of the polynomial functions detailed for the application of Hertz theory.

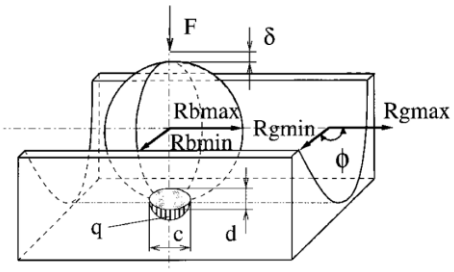

Fig. 4. Ball-groove interaction within the kinematic coupling.

Once the contact stresses and the corresponding deflections have been calculated, the positioning errors in the kinematic coupling can be determined. In the hypothesis that the distance between the balls does not change significantly, the deviations of the centroid of the coupling triangle $\delta_{\xi c}$ (ξ=*x*,*y*,*z*) can be calculated as the weighted average of the deflections of the balls that are obtained by application of Eq. 3.

Then, the calculation of the rotational errors is carried out: the estimation of the rotations ε_x and ε_y around the two corresponding axes requires to determine heights L and side orientation angles θ of the coupling triangle (Fig. 3) and leads to the following result (Eqs. 4 – 5):

$$\varepsilon_x = \frac{\delta_{z1}}{L_{1,23}}\cos\theta_{23} + \frac{\delta_{z2}}{L_{2,31}}\cos\theta_{31} + \frac{\delta_{z2}}{L_{3,12}}\cos\theta_{12} \tag{4}$$

$$\varepsilon_y = \frac{\delta_{z1}}{L_{1,23}}\sin\theta_{23} + \frac{\delta_{z2}}{L_{2,31}}\sin\theta_{31} + \frac{\delta_{z2}}{L_{3,12}}\sin\theta_{12} \tag{5}$$

The rotation error of the coupling around the *z*-axis (Eq. 6) is derived as the average of the rotations around the direction of *z*, with respect to the center of gravity of the coupling, calculated for each ball:

$$\varepsilon_z = \frac{\varepsilon_{z1} + \varepsilon_{z2} + \varepsilon_{z3}}{3} \tag{6}$$

Once the calculation of the rotation errors is completed, the translation errors δ_ξ (ξ=*x*,*y*,*z*) at any point around the coupling can be determined through the relation presented in Eq. 7:

$$\begin{bmatrix} \delta_x \\ \delta_y \\ \delta_z \\ 1 \end{bmatrix} = \begin{bmatrix} 1 & -\varepsilon_z & \varepsilon_y & \delta_{xc} \\ \varepsilon_z & 1 & -\varepsilon_x & \delta_{yc} \\ -\varepsilon_y & \varepsilon_x & 1 & \delta_{zc} \\ 0 & 0 & 0 & 1 \end{bmatrix} \cdot \begin{bmatrix} x - x_c \\ y - y_c \\ z - z_c \\ 1 \end{bmatrix} - \begin{bmatrix} x - x_c \\ y - y_c \\ z - z_c \\ 0 \end{bmatrix} \tag{7}$$

4 Analysis of the coupling in the laser-cutting machine

Payload of the cart is 450 kg. The mass of the cart, including the fixings and coupling elements, is equal to 300 kg. The inner part of the cart is used for the balancing of the external loads placed on the cart. The loading area is 1.1 m x 1.1 m. A 50 kg cast iron industrial weight was chosen as counterweight, 0.34 m x 0.2 m in plant view.

The first analysis concerned the study of deformations in the system, by considering pieces of different weight placed on the cart and located at its center of gravity. This analysis is necessary to assess that the required repeatability of 0.02 mm is achieved even in the case of maximum load. The results of the analysis are shown in Fig. 5. By considering a load of 4500 N, representative of the expected payload, the deformation at the center of gravity will be all-vertical, directed along the *z*-axis, and equal to about 0.006 mm. The stress ratio, i.e., the ratio between the contact pressure and the allowable Hertzian stress (equal to 1.5 times the ultimate tensile strength [11]), has been estimated at about 45%.

Subsequently, the point of application of the external load was changed. In this analysis, the center of gravity of the load was moved along the *y* axis, starting from ball 1 and approaching the other two balls (see Fig. 3 for reference). The results of the analysis are shown in Fig. 6. Ball 1 has a higher maximum stress ratio than the other two balls. The maximum value is reached when the load is applied directly on the ball (58%), whereas the contact stress is reduced at 34% when considering the midpoint between balls 2 and 3. As shown in Fig. 6, right, the trends related to balls 2 and 3 are overlapped, due to the applied load being equidistant to both spheres.

As far as the deformations are concerned, the overall deformation along the *z*-axis varies by the order of one thousandth of a millimeter, as shown in Fig. 6, left; however, it must be pointed out that the deformation changes locally on the three balls. By checking the individual balls, the maximum vertical deformation obtained at ball 1 was estimated equal to 0.0114 mm, therefore in any case lower than the required limit of 0.02 mm. The effect of rotation around *x* has also been verified. The rotation ε_x around the *x*-axis decreases as the external load approaches the center of gravity of the coupling. By using the maximum ε_x equal to 1.9e–5, obtained when the load was applied directly on ball 1, the overall displacement resulted equal to 0.0143 mm.

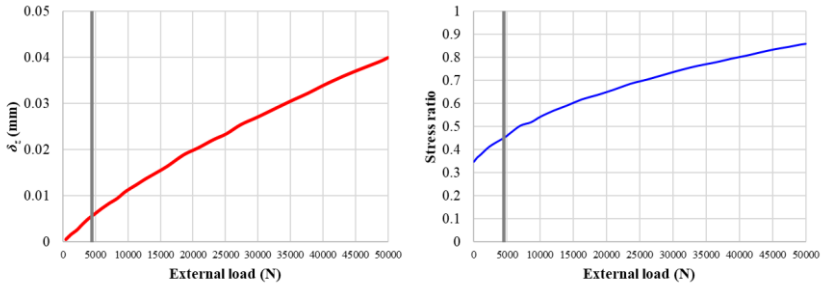

Fig. 5. Vertical deformation δ_z (left) and stress ratio (right) for different external load. Grey line refers to the expected load given by machine design specification.

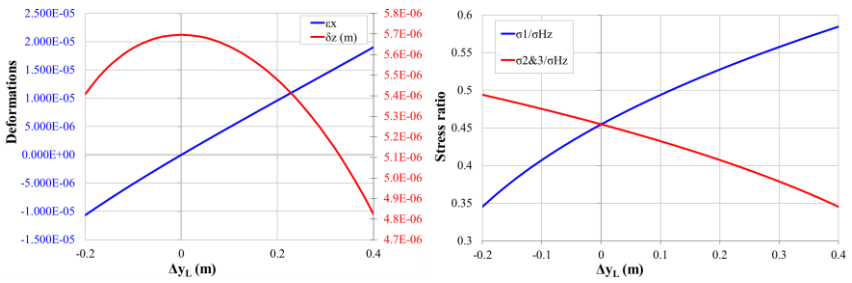

Fig. 6. Deformations (left) and stress ratios (right, for ball 1 and balls 2&3) for different positioning of the external load. Δy_L is the deviation from the centroid of the coupling, σHz is the allowable Hertzian stress.

Finally, the balancing of the system was evaluated, which can improve the precision of the coupling in the case of eccentric loads. Through the knowledge of the center of gravity of the cart and the positioning of the applied load, the field of action of the counterweight was estimated by balancing the moments acting on the system, producing the result represented in Fig. 7. The extent of the blue area depends on the dimensions and weight of the counterweight selected. Balancing leads to uniformity of the deformations on the spheres, thus canceling the consequent rotation errors that would be amplified by moving away from the center of gravity of the coupling. Compared to the case without balancing, the deformations δ_z and ε_x were always lower, yielding a maximum accuracy error of 0.0138 mm.

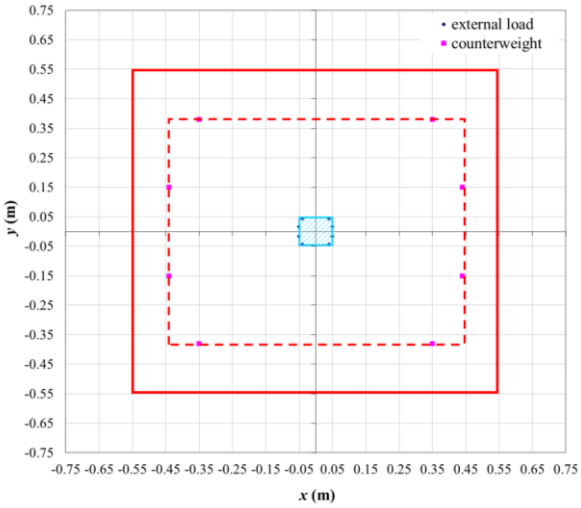

Fig. 7. Area of effect of the counterweight. Thick red line represents the cart, the red dashed line signals the area in which the counterweight must be confined to avoid obstacles. The area dotted in blue indicates where it is possible to locate the center of gravity of the load while perfect balance through the counterweight is still obtained.

5 Conclusion

The purpose of this paper was the verification of the precision guaranteed by a kinematic coupling with three grooves and spheres in a robotized laser-cutting machine, that requires a high level of accuracy.

A methodology used to estimate the positioning error was summarized, starting from the physical characteristics of the system and the application of Hertz's theory. The analysis was carried out considering typical loading conditions of the machine, that include unbalanced loads mounted on the cart in the working position. In each condition tested, the system has been shown to guarantee a positioning accuracy with errors lower than 0.02 mm at each point, as required by the application.

References

1. Vallance, R.R., Morgan, C., Slocum A.H.: Precisely positioning pallets in multi-station assembly systems. Precision Engineering, vol. 28, pp. 218–231 (2004).
2. Slocum, A.H.: Precision Machine Design, Prentice-Hall, Inc., Englewood Cliffs, New Jersey (1992).
3. Hale, L.C., Slocum, A.H.: Optimal design techniques for kinematic coupling. Precision Engineering, vol. 25, pp. 114–127 (2001).
4. Culpepper, M.L., Kartik, M.V., DiBiasio, C.: Design of integrated eccentric mechanisms and exact constraint fixtures for micron-level repeatability and accuracy. Precision Engineering, vol. 29, pp. 65–80 (2005).
5. Slocum, A.H.: Kinematic couplings: A review of design principles and applications. International Journal of Machine Tools and Manufacture, vol. 50, pp. 310–327 (2010).
6. Slocum, A.H.: Kinematic couplings for precision fixturing—Part I: Formulation of design parameters. Precision Engineering, vol. 10, pp. 85–931 (1988).
7. Slocum, A.H., Muller, L., Braunstein, D.: Flexural mount kinematic couplings and method. US Patent No. US5678944A (2005).
8. Prima Industrie S.p.A. Homepage, https://www.primaindustrie.com/it, last accessed 2022/01/31.
9. Slocum, A.H.: Design of three-groove kinematic couplings. Precision Engineering, vol. 14, pp. 67–76 (1992).
10. Hale, L.C.: Testing the limiting coefficient of friction with an adjustable 3-V kinematic coupling, vol. 64, pp. 200–209 (2020).
11. Roark, R.J., Young, W.C.: Formulas for Stress and Strain 5th ed., McGraw-Hill Book Co., New York (1975).